ORIGINAL ARTICLE

Near-infrared spectroscopy in resin transfer molding—determination of the degree of cure

Moritz Salzmann[1] · Wolfgang Märzinger[2] · Michael Teuchtmann[2] · Bharath Ravindran[1] · Ulrike Kirschnick[1] · Ewald Fauster[1]

Abstract

Near-infrared (NIR) spectroscopy is employed to directly monitor the degree of cure of composite material during the curing phase in the resin transfer molding (RTM) process. The composite material consists of natural fibers and an epoxy-amine resin system. The quantitative determination of the degree of cure, α, from the NIR spectra is realized by partial least square (PLS) regression in conjunction with various pre-treatments of the spectral data. As a reference, the degree of cure is determined by isothermal differential scanning calorimetry (DSC) experiments. The best PLS model that could be obtained for α is characterized by a determination coefficient of prediction (R²P) of 0.980 and root mean square error of prediction (RMSEP) of 4.4 %. While the spectra change during curing according to the literature for each RTM trial, significant differences can be observed between the spectra of different RTM trials. The reasons for this are discussed in detail. The findings show the potential of inline NIR spectroscopy for monitoring α in the RTM process.

Keywords Bio-composite · Degree of cure · Near-infrared spectroscopy · Resin transfer molding

1 Introduction

Fiber-reinforced polymer composites (FRPC) present an opportunity to fabricate optimized lightweight components. FRPCs consist of a fibrous reinforcement material embedded in a polymeric matrix, resulting in a material system combining both materials' advantages. FRPCs are increasingly used in the energy (wind power plants) and aerospace industries, among other sectors. The composite market was estimated at USD 100 billion in 2021 and is expected to grow at an annual rate of 5% until 2026 [1]. In addition to increasing demand, high-quality requirements are placed on components for aerospace and wind energy applications. The increasing requirements lead to growing demands on process stability.

There are several different process classes for the production of FRPC. One of these process classes is liquid composite molding (LCM), which includes RTM and vacuum-assisted resin infusion (VARI). All LCM procedures involve preparing a dry reinforcing structure, commonly referred to as a preform, followed by resin system infiltration with low viscosity and subsequent curing of the fully impregnated FRPC [2]. LCM processing allows the production of various components of varying complexity and size. It is widely employed due to its suitability for both easy prototype manufacturing and highly automated series production. The importance of process optimization [3] and reproducibility has increased [4], especially in series production. The growing trend toward automation in composite processing requires efficient inline monitoring techniques to ensure high levels of process stability and product quality [5]. Various promising techniques, such as ultrasonic [6, 7], dielectric analysis [8, 9], and direct current [10, 11], have been identified and are now in the focus of the research community [12].

Another promising method for inline monitoring is NIR spectroscopy. This technique avoids the need for sample preparation and enables the fast, non-destructive, and often contactless analysis of matter consisting of molecules. Light in the NIR spectral regime (750–2500 nm) creates overtone and combination vibrations of the molecules or functional

✉ Moritz Salzmann
moritz.salzmann@unileoben.ac.at

1 Processing of Composites Group,
Montanuniversität Leoben, Leoben, Austria

2 i-RED Infrarot Systeme GmbH, Linz, Austria

groups. The resulting NIR spectra can be used to determine chemical and physical parameters, such as concentration-related properties, by applying PLS regression. NIR spectroscopy has been used since the late 1950s in research laboratories [13–15] to understand the curing behavior of resins and for kinetic studies. However, its application for process monitoring in the composite industry is poorly documented. Today, the suitability of NIR spectroscopy for inline process monitoring is mainly investigated for prepreg production via the solvent route. Starting before impregnation, the sizing content on the fibers [16] and later in the process, matrix-related parameters such as the resin content [17, 18], volatile content [16, 17], soluble resin content [16, 19], the gel time [20], initiator content [21], and the ash content [22] have been determined for various textile and resin combinations. The quality of prepregs can also be determined during storage by NIR spectroscopy [23] to avoid using expired material. Although multiple parameters have been determined using NIR spectroscopy for prepreg manufacturing, there are hardly any studies on applying NIR spectroscopy in other FRPC processes. For the RTM process, however, we have already shown a high consistency in spectral changes of a single RTM trial over the curing process [24]. Even if, due to the small measuring range of a so-called micro-spectrometer, no peak directly involved in the curing process is affected, the occurring changes are significant enough to monitor the curing process.

NIR micro-spectrometers differ from full-scale spectrometers used for process monitoring in terms of their performance and costs. Depending on the spectrometer model used, they lack in covered wavelength range, resolution, and/or required measuring time per spectrum. At the same time, the costs are up to an order of magnitude lower.

In this study, the degree of cure of an epoxy-amine composite in the RTM process is monitored inline for the first time using NIR spectroscopy, considering process variations between trials. A previous study focused on the general possibility of measuring with NIR spectroscopy in the RTM process [24]. The deviations between the RTM trials have been intentionally neglected here, but their consideration is essential for efficient inline monitoring. Using a so-called micro-spectrometer raises questions regarding its suitability due to the limited wavelength range and increased measurement times. In addition, an approach for estimating the degree of cure at the beginning of the curing phase ($\alpha0$) is tested.

2 Experimental work

2.1 Materials

The composite produced consists of a natural fiber textile and an epoxy-amine matrix. The textile is a woven flax fiber 4/4 twill fabric (ampliTexTM 5042, Bcomp Ltd®, Fribourg, Switzerland). The preforms (270×269 mm) were stacked out of six layers of fabric each. Epinal IR 78.31/IH 77.11 (bto-epoxy GmbH, Amstetten, Austria) was used as the matrix resin.

2.2 RTM equipment

A square flat mold, hereafter referred to as a plate mold, was used for the RTM experiments. The cavity dimension was $270 \times 270 \times 4$ mm, and the mold was mounted on an LZT-OK-80-SO press (Langzauner GmbH, Lambrechten, Austria). The resin injection was done using a pressure pot.

2.3 RTM process

The RTM process is schematically shown in Fig. 1. The preform was dried in advance at 120 °C for 30 min and then immediately transferred into the preheated (60 °C) plate mold. The resin was thoroughly mixed by hand at room temperature and subsequently degassed until no more air bubbles were visible at the surface of the resin. Degassing took between 170 and 1053 s with an average duration of 400 s. The reason for this large span in

Fig. 1 Schematic drawing of the RTM process (left) and the NIR adapter (right)
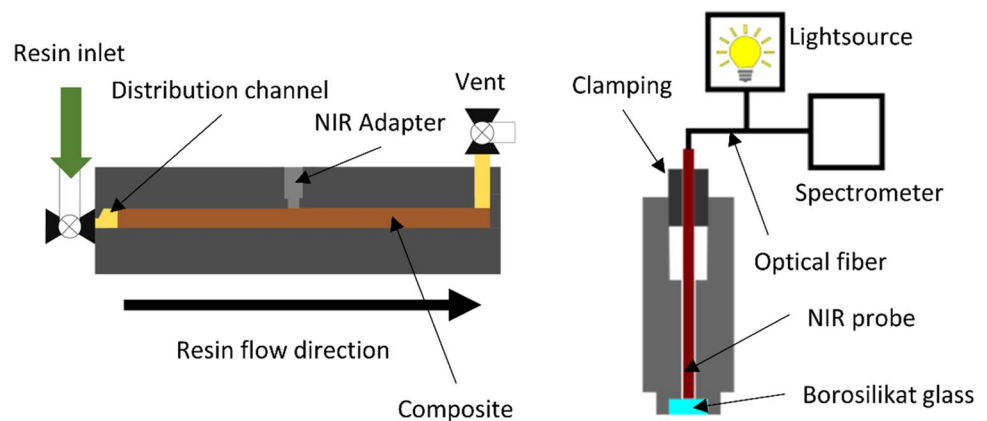
degassing time is the manual mixing, which adds strongly varying amounts of air to the resin despite all efforts for high reproducibility. The resin pot was placed in the pressure pot connected to the mold. The resin was injected with a pressure of 6 bar from the compressed air system. Once the resin had reached the two outlet tubes in the corners at the other end of the mold, the injection was stopped by closing these vents. The injection duration was between 655 and 1045 s, with an average injection duration of 752 s. The injection pressure was maintained for a further 60 min. Curing the resin was done isothermally at 60 °C for 180 min after closing the vents. After complete curing, the plate was demolded.

2.4 NIR equipment

The NIR measurements were carried out using a NIRONE S1.7 micro-spectrometer (Spectral Engines GmbH, Steinbach, Germany). It was connected to a NIR reflection probe and a halogen light source (AvaLight HAL S Mini) via a bifurcated fiber bundle (Y-cable), with all components coming from the same supplier (Avantes BV, Apeldoorn, Netherlands). The Y-cable consists of a single collection fiber (with a 400-μm core) and a bundle of thinner illumination fibers that meet at the cable junction to form a joint fiber bundle. This bundle extends to the tip of the NIR probe, with the central collection fiber surrounded by the illumination fibers. The probe was mounted in a self-constructed adapter in the center of the upper half of the mold (see Fig. 1). The adapter was designed with the process conditions in mind and consisted of a glass cover (5-mm borosilicate disk, Schott AG, Mainz, Germany) to protect the NIR probe and fixation for the probe.

2.5 NIR measurements

For the measurements, the light of the halogen source was forwarded to the probe via the illumination fibers and entered the cavity. The light reflected at the composite was then transferred back to the spectrometer by the collection fiber. NIR spectra were continuously recorded during resin injection and curing. The spectrometer measures in steps of 5 nm over a wavelength range from 1350 to 1650 nm, which results in 61 measuring points per spectrum. Each recorded spectrum is an average of 50 spectra, consisting of an average of 100 measurements at each wavelength. This results in a measurement time of 11 s per spectrum. The measurement series was started before injection and stopped after demolding. Spectra recorded outside the curing process were discarded based on their timestamp.

2.6 Reference measurements

The degree of cure was determined by isothermal DSC experiments (α_{DSC}) according to ISO 11357-5 (curing enthalpy) using the DSC1 (Mettler Toledo GmbH, Schwerzenbach, Switzerland) and the Mettler Toledo DSC software STARe for evaluation. Freshly mixed, uncured resin was weighed into a 40-μL aluminum crucible (10 ± 1 mg). The DSC measurements were conducted under a nitrogen atmosphere with a 50 mL/min gas flow at 60 °C for 240 min.

2.7 Statistical analysis

The recorded spectra and the reference values for α_{DSC} were used in PLS regression to develop and test a calibration model required for determining the degree of cure in the RTM process. The RTM experiments were split randomly into two sets, one for model calibration consisting of 12 trials and one for model validation with two trials. This procedure ensures that the PLS model is validated with data not contained in the model. The number of latent variables (LV), the determination coefficient of calibration (R²C), the determination coefficient of cross-validation (R²CV), determination coefficient of prediction (R²P), the root-mean-square error of calibration (RMSEC), root-mean-square error of cross-calibration (RMSECV), and root-mean-square error of prediction (RMSEP) are used as performance indicators of the developed PLS model. Several pre-treatments (see Table 1) to enhance the model quality were tested on the measured spectra. These pre-treatments include Standard Normal Variate (SNV), Smoothing (SM, done by a Savitzky-Golay-filter), First and Second Derivative (1. Deriv./2. Deriv., using a Savitzky-Golay-Filter), and Mean Center (MC). For the Savitzky-Golay filter, a filter width between 3 and 19 points was tested for each model. Cross-validation is done by continuous blocks, using data from one RTM trial as one block. All data evaluations were done with MATLAB (MathWorks Inc., Natick, USA) using the PLS Toolbox (Eigenvector Research Inc., Manson, USA).

Table 1 Overview of the pre-treatment of the spectra to improve the accuracy of the model when determining the degree of curing using NIR spectroscopy

Pre-treatments	Combinations with 2 pre-treatments	Combinations with 3 pre-treatments
SNV	SNV, SM	SNV, SM, MC
SM	SNV, 1. Deriv.	SNV, 1. Deriv., MC
1. Deriv.	SNV, 2. Deriv.	SNV, 2. Deriv., MC
2. Deriv.	SNV, MC	
MC		

3 Results

3.1 Determination of the degree of cure

Most reactive resin systems start to cure when the resin and hardener are mixed. The extent of curing depends primarily on the temperature. Many resin systems are, therefore, cured at elevated temperatures to shorten processing times and achieve better material properties [25]. The mold is typically preheated to curing temperature in the RTM process before the resin is injected. The increased temperature means that the resin starts to cure significantly as soon as it enters the mold; the pre-curing of the resin during its preparation at room temperature (mixing, degassing, etc.) is negligible. At the end of the injection phase, which coincides with the start of the actual curing phase, the resin will thus have a different degree of cure at each location in the mold. The duration of the injection phase, t_I, is the time the resin is injected before the vents at the back of the mold are closed.

From the isothermal DSC measurement, the degree of cure, α_{DSC}, is determined starting at 0% (representing the uncured resin) and tending towards 100% within the curing time of 240 min (see Fig. 2). The initially rapid curing slows down over time, as expected for an epoxy-amine resin. After 180 min, α has reached 99.9%, corresponding to almost complete curing and sufficient for potential applications. The remaining 0.1% are considered not to impact the material properties significantly.

As mentioned before, the curing during injection results in local differences in α at the end of the injection phase. For example, with an average t_I of 12 min 32 s, an α of about 19% is present at the outlet, while uncured resin is still injected at the inlet. Although these local differences in α decrease and almost vanish
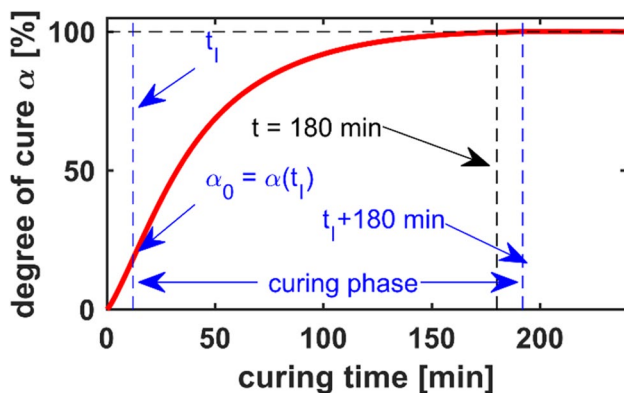

Fig. 2 Evolution of the degree of cure at 60 °C from DSC experiments. Shifts of the used range of α and curing time are marked in blue

at the end of the curing phase, they complicate the determination of the initial degree of cure α_0, i.e., the degree of cure at the beginning of the curing phase at the position below the NIR probe. Since the NIR probe in our setup is placed in the center of the mold (see Fig. 1), the initial degree of cure α_0 must be known to use the DSC data in the PLS regression as a reference and, thus, ultimately develop a model to predict α from the measured NIR spectra.

In principle, two parameters can be used to estimate α_0:

1. The injection duration, t_I, and
2. The time from reaching the NIR probe to the end of the injection, t_{reach}.

Attempts to correlate α_0 determined from dynamic DSC measurements with the duration of resin injection were unsuccessful. This is because residues of the natural fibers in the DSC samples influenced their weight and thus hindered a quantitative evaluation of the DSC experiments with sufficient accuracy. Instead, α_0 had to be estimated from the isothermal DSC curve (see Fig. 2) used as a reference for the PLS regression.

Assuming a linear flow front during injection, the mold is half-filled when the NIR probe is reached. Since the NIR probe is positioned in the center of the mold, the resin entering the mold at this moment should be located under the sensor at the end of the injection phase. Based on this assumption, the second option, t_{reach}, should be used. In reality, however, a linear flow front is not achieved. Even slight differences in the preform that occur during textile manufacturing, preform preparation, or positioning of the preform in the mold significantly impact the flow front's evolution during injection [26]. Considering that the injection time varies between 655 and 1045 s and the flow front reaches one vent earlier than the other in most trials, different evolutions of the flow front in the mold are apparent. The further flow of the resin, which reached the NIR probe first, is therefore unknown, and thus also α_0 of the resin under the NIR probe at the beginning of the curing phase. Since using the time t_{reach} introduces further variance to the reference data, which cannot be corrected, the authors decided to use the t_I to estimate the initial degree of cure α_0. This meant accepting that the resin's initial degree of cure α_0 under the NIR probe would be slightly overestimated (as it corresponds to the resin first injected at the beginning of the injection).

Therefore, to use α_{DSC} as reference data for the PLS regression and estimating α_0 from it, for each trial $\alpha_{DSC}(t_I)$ is set as α_0 and the curing phase is assumed to range from $\alpha_{DSC}(t_I)$ to $\alpha_{DSC}(t_I + 180\text{min})$. This results in α_0 values between 16.6 and 27.4% for the individual RTM trials.

Fig. 3 Representative NIR absorbance spectra of a natural fiber/epoxy amine composite during the curing process in RTM
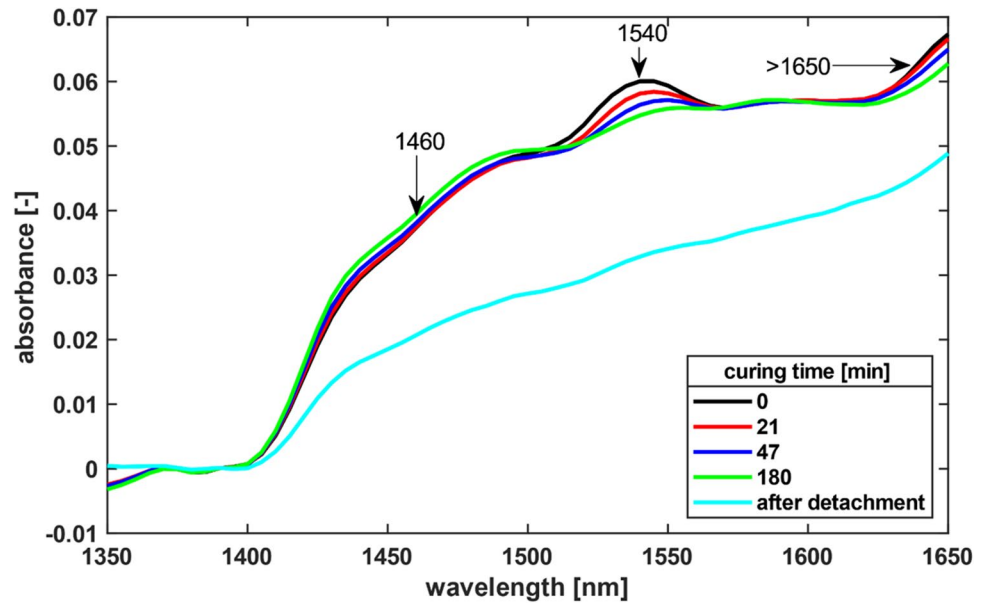

Table 2 Assignment of the observed absorption bands for chemical groups of a natural fiber/epoxy-amine composite between 1350 and 1650 nm

Peak position (nm)	Assigned functional group
1460	1st overtone of O-H stretching
1540	1st overtone of primary and secondary amine
~1650	1st overtone of terminal CH_2 stretching vibration of the epoxide ring CH, only left half of the peak visible

3.2 NIR spectra from the RTM process

In epoxy-amine resins, the oxirane rings of the epoxy monomers and the amine groups of the hardener act as reactive sites in the crosslinking reaction. During curing, the concentration of the oxirane rings and amine groups decreases while the concentration of hydroxy groups increases [14]. A selection of NIR spectra obtained during the curing process is shown in Fig. 3. As the measuring range of the NIRONE S1.7 spectrometer is limited between 1350 and 1650 nm, only three absorption bands are present (see Table 2 for their assignment). The absorption band of the hydroxy group at about 1460 nm is rather broad. It ranges from 1430 to 1500 nm and appears more as a shoulder than a clear peak. Literature assigns this peak, resulting from the conversion of the oxirane ring to a hydroxy group, between 1428 and 1438 nm [20, 27]. The peak at 1540 nm results from amine groups and decreases during resin curing [28, 29]. From the absorption of the oxirane ring (~1650 nm), only a small part is within the measuring range of the NIRONE S1.7. Literature assigns this peak between 1644 and 1656 nm [13, 30].
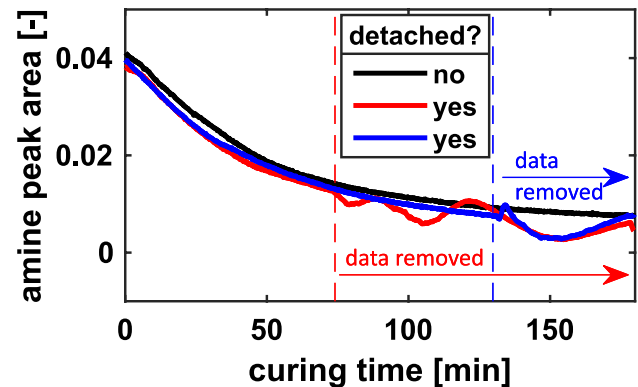

Fig. 4 Evolution of the normalized area under the amine peak during the curing process

Chemical shrinkage occurs as a result of the curing process. The shrinkage can cause the composite part to detach from the upper part of the mold due to gravity [31].

As the NIR probe is mounted to the upper part of the mold, detachment of the part inevitably leads to a separation of the NIR probe and the composite material. The detachment affects the spectral information collected after detachment (see Fig. 3, "144 (after detachment)"). The spectrum is flatter and no longer shows the bands of functional groups as before. Moreover, it changes significantly between 1350 and 1400 nm and differs from the other spectra, which overlap in this range. As these spectra would have a negative effect on the PLS regression models, they were not considered when creating the models. The amine peak was used as a reference to identify the detachment event in the spectra. To this end, the amine peak was baseline-corrected and integrated between 1455 and 1525 nm. The evolution of the peak area

in some RTM trials is shown representatively in Fig. 4. In all cases, it decreases at the beginning of the curing process. The area continuously decreases over time as long as the material remains in contact with the upper mold half and thus with the NIR probe (see Fig. 4, black). In the event of detachment, the curve no longer follows this continuous evolution.

Instead, the peak areas increase and decrease in a way that cannot be related to the ongoing curing process (see Fig. 4, red and blue). Therefore, if the peak area no longer follows the continuous decrease, the subsequent data cannot be considered in the analysis and must be removed. Four of the 14 plates detached during curing, with the earliest detachment occurring after 73 min (see Fig. 4, red). However, since the vast majority of the curing occurs at the early stages (see Fig. 2), after 73 min, an α of 87.8% could be reached. In all other cases, an α of 98.1% or higher was achieved before the detachment event.

3.3 PLS regression models for prediction of the degree of cure

The spectra are recorded at regular intervals. However, since the change in the degree of curing decreases over time (see Fig. 2), using all recorded spectra in the PLS regression would result in an overrepresentation of high degrees of curing. This would distort the regression. To ensure an even distribution of spectra across the degree of curing, the spectra were selected according to their corresponding degree of α_{DSC}. These corresponding degrees of curing are evenly distributed across the entire range of α_{DSC}. Doing so results in 223 to 267 spectra per RTM trial. Twelve RTM trials are used for model calibration, comprising 3070 spectra. The remaining two RTM trials are used for model validation, with a total of 531 spectra. Various pre-processing approaches were tested to improve spectral characteristics and reduce the influence of interfering factors. No outliers were identified in this step. The best PLS regression models found to determine α_{NIR} are summarized in Table 3.

The models that use either only the 1st Deriv. (model A) or MC (model B) exhibit comparable quality in terms of RMSECV and R²CV: both models have an RMSECV of 4.3% and an R²CV of 0.967 when using five LVs. Model A

shows a slight superiority in R²C and RMSEC with values of 0.983 and 3.0, respectively, compared to Model B with R²C = 0.982 and RMSEC = 3.1%. Despite similar results for RMSECV and RMSEP across all presented PLS models, model D stands out with an RMSECV of 4.7% and an RSMEP of 10.4%. A similar pattern is observed in the R^2 values, where model D has the highest R²C at 0.991, and an R²CV in the range of other models, but a relatively low R²P of 0.836. It is also noteworthy that model D, with nine LVs, requires many more LVs than the other models. Comparing the number of RTM trials with the required LVs for model D, it is suspected that the LVs describe the individual RTM trials rather than general changes in the spectra during curing.

Figure 5 plots the degree of cure predicted from cross-validation using model A against the reference values (α_{DSC}). The predicted degree of cure, α_{NIR}, correlates with the measured α_{DSC}. The main contribution to the RMSEs comes from differences between the RTM trials and not from fluctuations during one RTM trial. The α_{NIR} of an individual
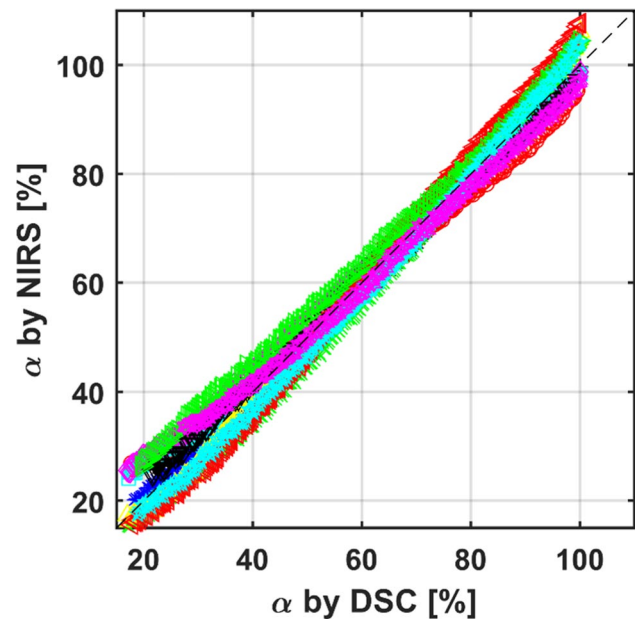

Fig. 5 Results of the cross-validation for the calibration dataset (model A)

Table 3 Summary of PLS calibration model statistics

PLS model	Preprocessing	LV	R^2C	R^2CV	R^2P	RMSEC (%)	RMSECV (%)	RMSEP (%)
A	1st Deriv (5 pt)	5	0.983	0.967	0.980	3.0	4.3	4.4
B	MC	5	0.982	0.967	0.971	3.1	4.3	5.6
C	SNV, 1st Deriv (7 pt)	5	0.980	0.965	0.985	3.3	4.4	4.4
D	2nd Deriv (19 pt)	9	0.991	0.963	0.836	2.2	4.7	10.4
E	SNV, 1st Deriv (7 pt), MC	4	0.981	0.960	0.990	3.2	4.7	4.6

RTM trial increases more or less linearly with α_{DSC}. This is supported by comparing the results of model A with linear fits of the individual RTM trials. The RTM trials' R^2 (linear fit) ranges from 0.963 to 0.999, while the RMSE (linear fit) ranges from 0.62 to 1.67%. The much smaller RMSE (linear fit) compared to the RMSEs of model A proves the consistency in the NIR spectra within one RTM trial and the difference between the RTM trials. At the end of the curing process, an α_{NIR} above 100% is predicted for some trials, which is physically impossible.

Using PLS model A, the degree of cure is predicted from the spectra of the validation dataset (see Fig. 6). The progression of α_{NIR} (Val-1_{NIR} and Val-2_{NIR}) is in relatively good correlation with the measured α_{DSC} (Ref$_{DSC}$). Significant deviations between α_{NIR} and α_{DSC} are only at the beginning of the curing process. For the validation trials, the predicted α_{NIR} at the beginning of the curing process is overestimated by 5.4% (Val-1_{NIR}) and 9.2% (Val-2_{NIR}), respectively. Within 15 min, the predicted degree of cure is approaching the measured degree of cure, and for the rest of the curing process, α_{NIR} deviates only between $\pm 2.5\%$ from α_{DSC}.

4 Discussion

Although the wavelength range of the NIR micro-spectrometer used is small (1350–1650 nm), the recorded spectra (see Fig. 3) contain information from all functional groups of the epoxy-amine resin system (oxirane ring, amine, and hydroxy groups) involved in the cur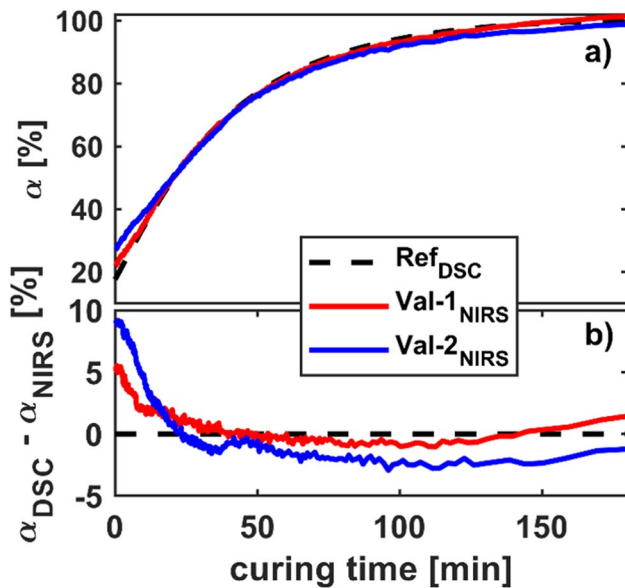ing process. Moreover, they show clear and consistent changes in the absorption bands during the curing process. These findings, which are promising for PLS regression, result in several PLS models with good predictive quality.

The predicted α_{NIR} of a single RTM trial shows a more or less linear increase when plotted against the measured α_{DSC} (see Fig. 5). The results of a linear fit support this finding, as outlined in Sect. 3.3. Despite this consistency within the individual RTM trials, no RMSECV lower than 4.3% could be achieved. This is due to the different measuring conditions between the trials, which we attribute to the variation in the (natural) fiber and the difficulty in determining α_0.

The textile affects the measuring conditions in several ways. Due to its structure, the actual measuring volume changes between each RTM trial. Since a natural fiber textile is used, fiber variations are more significant than for technical fibers. In addition, the moisture content changes between each RTM trial. The textile used is a twill 4/4 fabric, meaning the weft yarn runs over four warp yarns before passing under the following four warp yarns and coming up again (see Fig. 7). The undulations in the textile result in locally varying resin contents at the surface of the composite and thus in the measuring volume of the NIR probe. The measuring volume can be regarded as a cylinder, where the height is the distance between the upper half of the mold and the yarn of the first textile layer. The diameter of the cylinder depends on the NIR probe. The adapter used has a spot size of approximately 8 mm. This spot size is not enough to capture the repetitive structure of the textile several times and thus to average the effect of the locally varying resin content. Therefore, the measuring volume is expected to change between each RTM trial.

Another point concerning the textile is its natural origin (flax fibers). On the one hand, the differences between
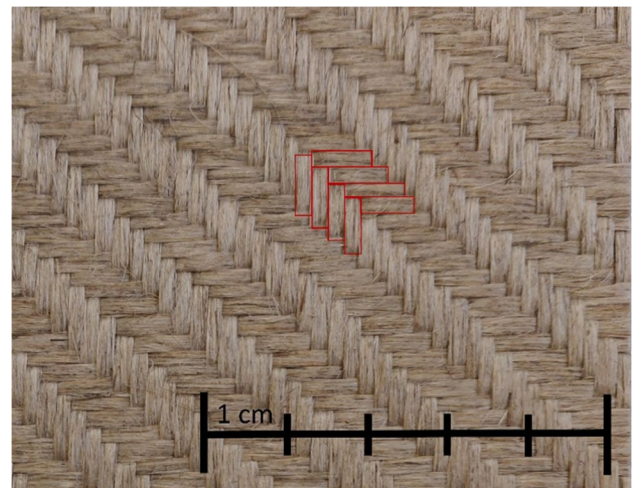

Fig. 6 Predicted degree of cure of the validation data (Val-1_{NIR} and Val-2_{NIR}) over the curing time using PLS model A (a) and the difference between predicted (α_{NIR}) and measured degree of cure (α_{DSC}) (b)

Fig. 7 Used natural fiber textile, a 4/4 fabric

the textiles are likely to be larger with a natural fiber than with a technical fiber. However, this effect is probably relatively small because the entire material comes from one role (batch). On the other hand, the curing process is affected by the moisture uptake of the natural fibers. Although the fibers are dried adequately before the processes, they reabsorb moisture from the air during handling and transferring the textile to the mold. Varying conditions in the lab and different handling times will result in slightly different moisture contents and thus affect the spectra.

The second aspect affecting the regression models' quality is the determination of α_0. The chosen path to estimate α_0 does not seem entirely off reality. Otherwise, the deviation would be more pronounced at lower degrees of cure in Fig. 5, resulting in poorer PLS models. The validation data (see Fig. 5) show a much more significant deviation from α_{DSC} at the beginning of the curing process than at a later stage. A more precise determination of α_0 would certainly increase model quality. Also, a shift of the NIR probe towards the injection gate could improve the quality of the models. (This approach was not realized in this study due to restrictions regarding the placement of the NIR probe in the RTM mold.) The resin is expected to be less cured during injection, and differences in the resin flow should have less influence on α_0.

Positioning the NIR probe above the distribution channel should solve both main issues: the changing measuring conditions and the problem of estimating the degree of cure at the beginning of the curing phase. On the one hand, the measured resin would be at tool temperature only for a reasonably short period, so an estimation of α_0 should be more accurate. On the other hand, the measuring volume would be constant, and the effects of the textile on the spectral data would, therefore, be reduced. Since the resin is least cured in the distribution channels, measuring at this position would also ensure that the rest of the part continues to cure, thus ensuring complete curing.

5 Conclusion

NIR spectroscopy was found to be a valuable tool for inline monitoring the degree of cure of a natural fiber/epoxy-amine composite in the RTM process. Despite the small measuring range of the micro-spectrometer used (1350–1650 nm), all functional groups involved in the curing process have absorption bands in this spectral regime. In addition, the absorption bands show clear and consistent changes with increasing degrees of cure, which were used as the basis for developing PLS regression models to determine the degree of cure quantitatively.

Several PLS models with good predictive quality that can determine α with reasonable accuracy have been developed.

The models show high consistency within the individual RTM experiments, but variations between the trials prevent a better model quality. These variations are mainly related to the natural fiber textile and the estimation of α_0 at the beginning of the curing phase. The validation data show deviations from the reference data but converge towards the expected α as curing progresses.

Overall, the NIR micro-spectrometer used in this study proved a valuable and cost-effective tool for inline monitoring the degree of cure in composite manufacturing by RTM. To fully leverage the potential of this technology, future research could focus on a more reliable determination of α_0 and repositioning the NIR probe at a more suitable location.

Declarations

Competing interests The authors declare no competing interests.

References

1. Estin ea (2022) JEC observer. Current trends in the global composites industry 2021–2026, Paris

2. Mallick PK (2007) Fiber-reinforced composites. Materials, manufacturing, and design, 3rd ed., expanded and rev. ed. CRC Press, Boca Raton FL

3. Struzziero G, Skordos AA (2019) Multi-objective optimization of resin infusion. Adv Manufacturing: Polym Compos Sci 5(1):17–28. https://doi.org/10.1080/20550340.2019.1565648

4. Konstantopoulos S, Hueber C, Antoniadis I et al (2019) Liquid composite molding reproducibility in real-world production of fiber reinforced polymeric composites: a review of challenges and solutions. Adv Manufacturing: Polym Compos Sci 5(3):85–99. https://doi.org/10.1080/20550340.2019.1635778

5. Hueber C, Konstantopoulos S, Hergan P, Höfler J, Horejsi K, Schledjewski R (2017) Influence of cure monitoring on the curing cycle time and the associated economic impact. J Mineral Metal Mater Eng 3:58–63

6. Fomitchov PA, Kim YK, Kromine AK et al (2002) Laser ultrasonic array system for real-time cure monitoring of polymermatrix composites. J Compos Mater 36(15):1889–1901. https://doi.org/10.1177/0021998302036015245

7. Schmachtenberg E, zur Schulte Heide J, Töpker J (2005) Application of ultrasonics for the process control of resin transfer moulding (RTM). Polym Test 24(3):330–338. https://doi.org/10.1016/j.polymertesting.2004.11.002

8. Yenilmez B, Murat Sozer E (2009) A grid of dielectric sensors to monitor mold filling and resin cure in resin transfer molding. Compos Part A: Appl Sci Manufac 40(4):476–489. https://doi.org/10.1016/j.compositesa.2009.01.014

9. Lee DG, Kim HG (2004) Non-isothermal in situ dielectric cure monitoring for thermosetting matrix composites. J Compos Mater 38(12):977–993. https://doi.org/10.1177/0021998304040563

10. Hergan P (2019) Entwicklung einer modellbasierten Fertigungstechnik zur intrinsischen Herstellung von hybriden Verbundwerkstoffen. Dissertation

11. Garschke C, Weimer C, Parlevliet PP et al (2012) Out-of-autoclave cure cycle study of a resin film infusion process using in situ process monitoring. Compos Part A: Appl Sci Manufac 43(6):935–944. https://doi.org/10.1016/j.compositesa.2012.01.003

12. Konstantopoulos S, Fauster E, Schledjewski R (2014) Monitoring the production of FRP composites: a review of inline sensing methods. Express Polym Lett 8(11):823–840. https://doi.org/10.3144/expresspolymlett.2014.84

13. Goddu RF, Delker DA (1958) Determination of terminal epoxides by near- infrared spectrophotometry. Anal Chem 30:2013–2016

14. Billaud C, Vandeuren M, Legras R et al (2002) Quantitative analysis of epoxy resin cure reaction: a study by near-infrared spectroscopy. Appl Spectrosc 56(11):1413–1421. https://doi.org/10.1366/00037020260377706

15. Mijcovic J, Andjelic S (1995) A study of reaction kinetics by near-infrared spectroscopy. 1. Comprehensive analysis of a model epoxy/amine system. Macromolecules 28:2787–2796

16. Jiang B, Huang Y (2007) Near infrared spectroscopy for on-line monitoring of alkali-free cloth /phenolic resin prepreg during manufacture. IJMS 8(6):541–552. https://doi.org/10.3390/i8060541

17. Li W, Huang YD, Liu L et al (2006) On-line monitoring of resin content and volatile content in carbon/phenolic resin prepreg cloth by near-infrared-spectroscopy. Polym Polym Compos 14:537–543

18. Jiang B, Huang YD (2008) Quality inspection of laid fabric epoxy resins prepreg by near infrared spectroscopy. Compos Part A: Appl Sci Manufac 39(5):712–717. https://doi.org/10.1016/j.compositesa.2008.02.009

19. Li W, Huang YD, Chen P (2008) Use of near-infrared spectroscopy for on-line monitoring the quality of prepreg cloth. Adv Compos Lett 17(2):096369350801700. https://doi.org/10.1177/096369350801700201

20. Liu Q-F, Li D, Zeng Y-D et al (2021) Determination of gel time of prepreg in copper clad laminate industry by near infrared spectroscopy. J Near Infrared Spectrosc 29(1):5–10. https://doi.org/10.1177/0967033520963799

21. Liu Q, Li D, Guan C (2022) Analysis of initiator content of prepreg by near-infrared spectroscopy. Rev Anal Chem 41(1):74–82. https://doi.org/10.1515/revac-2022-0035

22. Wu Y-H, Li D (2022) Determination of ash content in silicon dioxide filled epoxy-phenolic prepreg using near infrared spectroscopy. J Near Infrared Spectrosc 30(4):227–233. https://doi.org/10.1364/JNIRS.30.000227

23. Salzmann M, Teuchtmann M, Schledjewski R (2023) Determination of the glass transition temperature of an epoxy prepreg by near infrared spectroscopy. Polym Test 125:108111. https://doi.org/10.1016/j.polymertesting.2023.108111

24. Salzmann M, Blößl Y, Todorovic A et al (2021) Usage of near-infrared spectroscopy for inline monitoring the degree of curing in RTM processes. Polymers 13(18). https://doi.org/10.3390/polym13183145

25. Singh JIP, Singh S, Dhawan V (2018) Effect of curing temperature on mechanical properties of natural fiber reinforced polymer composites. J Nat Fibers 15(5):687–696. https://doi.org/10.1080/15440478.2017.1354744

26. Bickerton S, Advani SG (1999) Characterization and modeling of race-tracking in liquidcomposite molding processes. Compos Sci Technol 59(15):2215–2229. https://doi.org/10.1016/S0266-3538(99)00077-9

27. Mijovic J, Andjelic S, Yee CFW et al (1995) A study of reaction kinetics by near-infrared spectroscopy. 2. Comparison with dielectric spectroscopy of model and multifunctional epoxy/amine systems. Macromolecules 28(8):2797–2806. https://doi.org/10.1021/ma00112a027

28. Lohman FH, Norteman E Jr (1963) Determination of primary and secondary aliphatic amines by near-infrared spectrophotometry. Anal Chem 35:707–711

29. Mijović J, Andjelić S, Kenny JM (1996) In situ real-time monitoring of epoxy/amine kinetics by remote near infrared spectroscopy. Polym Adv Technol 7(1):1–16. https://doi.org/10.1002/(SICI)1099-1581(199601)7:1<1:AID-PAT480>3.0.CO;2-N

30. Chike KE, Myrick ML, Lyon RE et al (1993) Raman and near-infrared studies of an epoxy resin. Appl Spectrosc 47(10):1631–1635. https://doi.org/10.1366/0003702934334714

31. Ramos JA, Pagani N, Riccardi CC et al (2005) Cure kinetics and shrinkage model for epoxy-amine systems. Polymer 46(10):3323–3328. https://doi.org/10.1016/j.polymer.2005.02.069